

Cite this: *Dalton Trans.*, 2013, **42**, 9263

Chiral and achiral (imino)phenoxy-based cationic group 4 non-metallocene complexes as catalysts for polymerization of renewable α -methylene- γ -butyrolactone†

Ravikumar R. Gowda and Eugene Y.-X. Chen*

Protonolysis of $M(\text{Bn})_4$ ($M = \text{Zr, Ti}$; $\text{Bn} = \text{benzyl}$) with equimolar 2,4-di-*tert*-butyl-6-[(2,6-diisopropylphenyl-imino)methyl]phenol [(2,6-^{*i*}Pr₂C₆H₃)N=C(3,5-^{*t*}Bu₂C₆H₂)OH] in toluene at -30 °C to 25 °C cleanly affords the corresponding achiral (imino)phenoxy-tribenzyl complexes, [(2,6-^{*i*}Pr₂C₆H₃)N=C(3,5-^{*t*}Bu₂C₆H₂)O]Zr-(Bn)₃ (**1**) and [(2,6-^{*i*}Pr₂C₆H₃)N=C(3,5-^{*t*}Bu₂C₆H₂)O]Ti(Bn)₃ (**2**). A chiral dibenzyl complex **3** incorporating the unsymmetric, tetradentate amino(imino)bis(phenoxy) ligand, [2,4-Br₂C₆H₂(O)(6-CH₂(NC₅H₉))-CH₂N=CH(2-adamantyl-4-MeC₆H₂O)]Zr(Bn)₂ (**3**), has also been prepared using the same protonolysis protocol. Abstractive activation of **1** with B(C₆F₅)₃·THF in CD₂Cl₂ at room temperature (RT) affords clean, quantitative formation of the corresponding zirconium cation [(2,6-^{*i*}Pr₂C₆H₃)N=C(3,5-^{*t*}Bu₂C₆H₂)O]Zr-(Bn)₂(THF)]⁺[BnB(C₆F₅)₃]⁻ (**4**). Likewise, benzyl abstraction of **2** with B(C₆F₅)₃·THF in CD₂Cl₂ at RT generates the cationic titanium complex [(2,6-^{*i*}Pr₂C₆H₃)N=C(3,5-^{*t*}Bu₂C₆H₂)O]Ti(Bn)₂(THF)]⁺[BnB(C₆F₅)₃]⁻ (**5**), accompanied by a small amount of decomposed species as a result of C₆F₅ transfer. The dibenzyl cations **4** and **5** have been characterized spectroscopically, and their structures have been confirmed by single crystal X-ray diffraction analysis. Characteristics of the coordination polymerization of renewable α -methylene- γ -butyrolactone monomers by the cationic catalysts derived from achiral complexes **1** and **2** as well as chiral complex **3** have been investigated, representing the first study of such polymerization by non-metallocene catalysts.

Received 15th February 2013,

Accepted 7th March 2013

DOI: 10.1039/c3dt50430a

www.rsc.org/dalton

Introduction

The prospect of using naturally occurring or biomass-derived renewable resources to substitute depleting petroleum-based raw materials in large commodity markets, such as plastics, fibers, and fuels, have been explored recently.^{1–3} In this context, several compounds containing an α -methylene- γ -butyrolactone moiety were found and isolated from various plants.⁴ The best characterised tulipaline is tulipaline A, or α -methylene- γ -butyrolactone (MBL), found in tulips,^{4,5} which is the most studied monomer of this family. MBL consists of a five-membered lactone ring, exhibits structural features similar to those of methyl methacrylate (MMA), and polymerizes in a similar manner too (*i.e.*, vinyl addition without ring-opening of the lactone). Poly(α -methylene- γ -butyrolactone) (PMBL) has good durability, a high refractive index of 1.540,⁶

and a high T_g of 195 °C (for atactic polymer).⁷ MBL units present in various copolymers and blends have good optical properties as well as resistance to heat, weathering, scratches, and solvents.⁸ Another monomer considered in this area of study is the γ -methyl derivative of MBL, γ -methyl- α -methylene- γ -butyrolactone (MMBL), which can be readily prepared *via* a two-step process from the biomass-derived levulinic acid.^{9,10} MBL and MMBL are of special interest in exploring the prospects of substituting the petroleum-based methacrylate monomers for specialty chemicals production.¹¹ Various types of polymerization processes have been adopted to polymerize MBL to low to high molecular weight (MW) polymers, proceeding through radical polymerization,^{7,12} anionic polymerization,⁷ group-transfer polymerization,¹³ coordination polymerization with metallocene complexes;¹⁴ MBL has been copolymerized with various comonomers^{12a} such as MMA,¹⁵ styrene,^{12e,16} methoxystyrene,¹⁷ and vinyl thiophenes.¹⁸ The polymerization of MMBL has not been studied extensively as compared to MBL; nevertheless, it has also been polymerized by free-radical emulsion polymerization^{6,19} as well as radical, anionic, and group-transfer polymerization methods.²⁰

Department of Chemistry, Colorado State University, Fort Collins,

Colorado 80523-1872, USA. E-mail: eugene.chen@colostate.edu

†CCDC 924151 (4) and 924152 (5). For crystallographic data in CIF or other electronic format see DOI: 10.1039/c3dt50430a

We have developed several catalyst systems for rapid, controlled, or stereoselective polymerization of such monomers, including bifunctional silicon propagators for living polymerization of MBL and MMBL,²¹ half-sandwich indenyl rare-earth metal dialkyls with exceptional activity for the polymerization of MMBL in DMF,²² alane-based classical and frustrated Lewis pairs for rapid polymerization of MBL and MMBL into high MW polymers,²³ a dinuclear silylium-enolate bifunctional catalyst with high activity and stereoselectivity (at low temperature) for the polymerization of MMA and MMBL,²⁴ and *N*-heterocyclic carbenes for rapid organocatalytic polymerization of MMBL and MBL.²⁵ Most recently, we have developed the first stereoselective polymerization of the β -methyl derivative, β -methyl- α -methylene- γ -butyrolactone (β MMBL), into stereo-defect-free polymers²⁶ by single-site chiral metallocene catalysts that are known to promote stereospecific coordination polymerization of polar vinyl monomers.²⁷

Applications of group 4 non-metallocene catalysts in α -olefin polymerization have been well documented.²⁸ Selected notable examples include: sterically hindered chelating phenoxy titanium and zirconium complexes²⁹ for living polymerization of 1-hexene,³⁰ 2,2'-ethylenebis(*N,N'*-(triisopropylsilyl)anilino)zirconium complexes for living polymerization of α -olefin,³¹ bis(pentafluorophenylamido)zirconium benzyl complexes for ethylene polymerization,³² a C_2 -symmetric amine bis(phenolate)zirconium benzyl catalyst for iso-specific living polymerization of 1-hexene,³³ an amine bis(phenolate)titanium benzyl catalyst for block copolymerization of α -olefins,³⁴ amine bis(phenolate)zirconium dibenzyl complexes,³⁵ extremely active [ONXO]-type zirconium and hafnium dibenzyl complexes of amine bisphenolates (X = N, O, S),³⁶ group 4 complexes of an amine bis(phenolate) ligand featuring a THF molecule as well as furan sidearm donors,³⁷ and zirconium and titanium diamine bis(phenolate) catalysts³⁸ utilized for 1-hexene polymerization. In 2005, Kol and co-workers employed zirconium dibenzyl complexes of chiral salan ligands for iso-specific polymerization of 1-hexene and 4-methyl-1-pentene as well as cyclopolymerization of 1,5-hexadiene,³⁹ titanium and zirconium dibenzyl complexes of robust salophan ligands in 1-hexene polymerization,⁴⁰ salan zirconium complexes for production of highly isotactic poly(vinylcyclohexane),⁴¹ and C_1 -symmetric [ONNO]-type salan zirconium complexes in 1-hexene polymerization.⁴² More recently, Kol *et al.* have reported the use of titanium dibenzyl complexes incorporating salalen (*i.e.*, half-salan/half-salen) ligands for the synthesis of highly isotactic polypropylene with a melting transition temperature (T_m) of 169.9 °C, the highest T_m reported for "as prepared" (not extracted or annealed) isotactic polypropylene produced by either heterogeneous or homogeneous catalysts to date.⁴³ Okuda and co-workers reported group 4 complexes supported by [ONNO]-type bis(*o*-aminophenolato) ligands for α -olefin polymerization.⁴⁴ Waymouth and co-workers developed hafnium and zirconium dibenzyl bis(phenolate)ether complexes for propylene polymerization.⁴⁵ Aryloxy, imino and bis(imino)phenoxides of group 4 alkoxides are also active for ring-opening polymerization of cyclic esters

(ϵ -caprolactone, δ -valerolactone, β -butyrolactone, and lactides) as well as ethylene and propylene polymerization.⁴⁶

In view of the exciting benefits of MBL and MMBL monomers and their corresponding polymers as well as the outstanding performances of amine bis(phenolates) and salalen complexes of group 4 dibenzyl complexes in the polymerization of 1-hexene and propylene, we were intrigued by the prospect of such non-metallocene complexes being effective catalysts for coordination polymerization of the renewable butyrolactone-based vinyl monomers such as MBL and MMBL. However, to the best of our knowledge, there were no reports on the utilization of such catalysts for this polymerization catalysis. In the present contribution, we report syntheses and characterization of group 4 benzyl complexes supported by imino(phenolate)⁴⁷ and salalen⁴³ ligands as well as the first structural characterization of group 4 dibenzyl cationic complexes⁴⁸ that incorporate the imino(phenolate) ligand and their polymerization activity towards MMBL, MBL and MMA.

Experimental

Materials, reagents, and methods

All syntheses and manipulations of air- and moisture-sensitive materials were carried out in flamed Schlenk-type glassware on a dual-manifold Schlenk line, on a high-vacuum line, or in an inert gas (Ar or N₂)-filled glovebox. NMR-scale reactions were conducted in Teflon-valve-sealed J. Young-type NMR tubes. HPLC-grade organic solvents were first sparged extensively with N₂ during filling 20 L solvent reservoirs and then dried by passage through activated alumina (for Et₂O, THF, and CH₂Cl₂) followed by passage through Q-5 supported copper catalyst (for toluene and hexanes) stainless steel columns. Benzene-d₆ and toluene-d₈ were dried over sodium/potassium alloy and vacuum-distilled or filtered, whereas CD₂Cl₂ and CDCl₃ were dried over activated Davison 4 Å molecular sieves. NMR spectra were recorded on a Varian Inova 300 (300 MHz, ¹H; 75 MHz, ¹³C; 282 MHz, ¹⁹F) or 400 MHz spectrometer. Chemical shifts for ¹H and ¹³C spectra were referenced to internal solvent resonances and are reported as parts per million relative to SiMe₄, whereas ¹⁹F NMR spectra were referenced to external CFCl₃. Elemental analyses were performed by Robertson Microlit Laboratories, Madison, NJ.

Triethylamine, 3,5-dibromosalicylaldehyde, paraformaldehyde, and zirconium(IV) chloride were purchased from Alfa Aesar Chemical Co. Benzyl magnesium chloride, 2-(aminomethyl)piperidine, 3,5-di-*tert*-butyl-2-hydroxybenzaldehyde, and titanium(IV) chloride were purchased from Sigma-Aldrich Chemical Co. and used as received. Formaldehyde (36–38% aqueous solution) was purchased from Mallinckrodt Chemicals. Tetrabenzyltitanium and tetrabenzylzirconium were prepared according to published procedures⁴⁹ and used shortly after. Ligands 3-adamantyl-2-hydroxy-5-methylbenzaldehyde,⁵⁰ 2-(bromomethyl)-4,6-dibromophenol,⁴³ and 2,4-di-*tert*-butyl-6-((2,6-diisopropylphenylimino)methyl)phenol [(2,6-ⁱPr₂C₆H₃)-N=C(3,5-^tBu₂C₆H₂)OH]⁵¹ were synthesized according to

published procedures. Methyl methacrylate (MMA) was purchased from Sigma-Aldrich Chemical Co., while α -methylene- γ -butyrolactone (MBL) and γ -methyl- α -methylene- γ -butyrolactone (γ -MMBL) were purchased from TCI America. These monomers were first degassed and dried over CaH₂ overnight, followed by vacuum distillation; MMA was further purified by titration with neat tri(*n*-octyl)aluminum to a yellow end point and distillation under reduced pressure. The purified monomers were stored in brown bottles inside a glovebox freezer at -30 °C. Butylated hydroxytoluene (BHT-H, 2,6-di-*tert*-butyl-4-methylphenol) was purchased from Alfa Aesar Chemical Co. BHT-H was recrystallized from hexanes prior to use. Tris(pentafluorophenyl)borane, B(C₆F₅)₃, was obtained as a research gift from Boulder Scientific Co. and was further purified by sublimation. B(C₆F₅)₃·THF was prepared by addition of THF to a toluene solution of the borane at ambient temperature, followed by removal of the volatiles and drying under vacuum.

Synthesis of 2-[(aminomethyl)piperidine]-4-methyl-6-adamantylphenol

2-(Aminomethyl)piperidine (0.84 g, 7.39 mmol) was added to a solution of 3-adamantyl-2-hydroxy-5-methylbenzaldehyde (2.00 g, 7.39 mmol) in benzene (20 mL). The resulting mixture was refluxed for 8 h, after which the solvent was removed under vacuum to give a yellow solid; yield: 2.41 g (88%). ¹H NMR (CDCl₃, 23 °C): δ 13.62 (br, 1H, OH), 8.32 (s, 1H, CH=N), 7.36 (s, 1H, Ar-H), 7.07 (d, *J* = 2.0 Hz, 1H, Ar-H), 3.67 (m, 1H, CH₂N), 3.38 (m, 1H, CH₂N), 3.05 (m, 1H, CHNH), 2.88 (m, 1H, CH₂NH), 2.65 (m, 1H, CH₂NH), 2.28 (s, 3H, Ar-CH₃), 2.23 (bs, 1H, NH), 2.17 (m, 6H, adamantyl), 2.08 (bs, 3H, adamantyl), 1.83 (m, 2H, CH₂), 1.78 (bs, 6H, adamantyl), 1.71 (m, 1H, CH₂), 1.64 (m, 1H, CH₂), 1.40 (m, 1H, CH₂), 1.26 (m, 1H, CH₂).

Synthesis of 2,4-Br₂C₆H₂(OH)(6-CH₂(NC₅H₉))CH₂N=CH-(2-adamantyl-4-MeC₆H₂OH)

A solution of 2-(bromomethyl)-4,6-dibromophenol (2.06 g, 5.97 mmol) in THF (30 mL) was added dropwise to a solution of 2-(aminomethyl)piperidine-4-methyl-6-adamantylphenol (2.19 g, 5.97 mmol) and triethylamine (14 mL) in THF (30 mL) and stirred for 5 h. The solid that formed was filtered off and the solvent was removed under vacuum. The crude product was re-crystallized from cold methanol yielding the titled ligand as a yellow solid; yield: 3.76 g (93%). ¹H NMR (CDCl₃, 23 °C): δ 8.23 (s, 1H, CH=N), 7.53 (d, *J* = 2.2 Hz, 1H, Ar-H), 7.08 (d, *J* = 1.7 Hz, 1H, Ar-H), 7.03 (d, *J* = 2.0 Hz, 1H, Ar-H), 6.86 (s, 1H, Ar-H), 4.23 (d, *J* = 14.7 Hz, 1H, Ar-CH₂), 3.94 (m, 1H, Ar-CH₂), 3.76–3.49 (m, 2H, CH₂N=CH), 3.03–2.78 (m, 2H, CH₂N), 2.78–2.57 (m, 1H, CHN), 2.28 (s, 3H, Ar-CH₃), 2.16 (m, 6H, adamantyl), 2.08 (bs, 3H, adamantyl), 1.93–1.82 (m, 2H, CH₂), 1.78 (bs, 6H, adamantyl), 1.69–1.62 (m, 1H, CH₂), 1.43 (s, 1H, CH₂), 1.21–1.05 (m, 2H, CH₂). Anal. Calcd for C₃₁H₃₈Br₂N₂O₂: C, 59.06; H, 6.08; N, 4.44. Found: C, 59.18; H, 6.19; N, 4.34.

Synthesis of [(2,6-¹Pr₂C₆H₃)N=C(3,5-^tBu₂C₆H₂)O]Zr(Bn)₃ (1)

A solution of (2,6-¹Pr₂C₆H₃)N=C(3,5-^tBu₂C₆H₂)OH (1.00 g, 2.54 mmol) in toluene (15 mL) and Zr(Bn)₄ (1.15 g, 2.54 mmol) in toluene (15 mL) was pre-cooled at -30 °C inside the glovebox for 12 h. After mixing the solutions, orange precipitates instantly appeared. Stirring continued for 24 h at ambient temperature, the reaction mixture was filtered to afford the crude product. This orange product was further dried for 1 h under reduced pressure; yield: 1.50 g (78%). ¹H NMR (C₆D₆, 23 °C): δ 8.13 (s, 1H, CH=N), 7.76 (s, 1H, Ar-H), 7.13–6.87 (m, 21H, Ar-H, C₇H₈), 2.69–2.56 (m, 2H, Ar-CH(CH₃)₂), 2.26 (bs, 6H, Ar-CH₂-Zr), 2.11 (s, 3H, C₇H₈), 1.52 (s, 9H, Ar-C(CH₃)₃), 1.24 (s, 9H, Ar-C(CH₃)₃), 1.22 (d, *J* = 6.8 Hz, 6H, Ar-CH(CH₃)₂), 0.90 (d, *J* = 6.7 Hz, 6H, Ar-CH(CH₃)₂). ¹³C NMR (C₆D₆, 23 °C): δ 172.5 (Ar-CH=N), 160.2 (Ar-O-Zr), 152.1 (Ar-N=CH), 141.8 (Ar-C(CH₃)₃), 140.9 (Ar-C(CH₃)₃), 140.6 (Ar-CH₂-Zr), 138.3 (Ar-CH(CH₃)₂), 137.9 (C₇H₈), 132.2 (Ar-C), 130.0 (Ar-C), 129.4 (Ar-C), 129.3 (C₇H₈), 129.1 (Ar-C), 128.5 (C₇H₈), 127.4 (Ar-C), 125.7 (C₇H₈), 124.6 (Ar-C), 123.8 (Ar-C), 122.7 (Ar-C), 72.6 (Ar-CH₂-Zr), 35.4 (Ar-C(CH₃)₃), 34.3 (Ar-C(CH₃)₃), 31.4 (Ar-C(CH₃)₃), 30.2 (Ar-C(CH₃)₃), 29.3 (Ar-CH(CH₃)₂), 25.3 (Ar-CH(CH₃)₂), 23.2 (Ar-CH(CH₃)₂), 21.4 (C₇H₈). Anal. Calcd for C₄₈H₅₉NOZr·2C₇H₈: C, 79.09; H, 8.03; N, 1.49. Found: C, 78.94; H, 8.09; N, 1.85.

Synthesis of [(2,6-¹Pr₂C₆H₃)N=C(3,5-^tBu₂C₆H₂)O]Ti(Bn)₃ (2)

A solution of [(2,6-¹Pr₂C₆H₃)N=C(3,5-^tBu₂C₆H₂)OH] (1.00 g, 2.54 mmol) in toluene (15 mL) and Ti(Bn)₄ (1.04 g, 2.54 mmol) in toluene (15 mL) was pre-cooled at -30 °C inside the glovebox for 12 h. After mixing the solutions, a red solution appeared instantly. Stirring continued for 24 h at RT, after which the solvent was removed under reduced pressure to afford a red solid. This residue was further purified by crystallization from toluene at -30 °C; yield: 1.40 g (77%). ¹H NMR (C₆D₆, 23 °C): δ 8.21 (s, 1H, CH=N), 7.79 (s, 1H, Ar-H), 7.13–6.85 (m, 21H, Ar-H, C₇H₈), 3.51 (bs, 6H, Ar-CH₂-Ti), 2.41–2.29 (m, 2H, Ar-CH(CH₃)₂), 2.11 (s, 3H, C₇H₈), 1.58 (s, 9H, Ar-C(CH₃)₃), 1.24 (s, 9H, Ar-C(CH₃)₃), 1.11 (d, *J* = 6.7 Hz, 6H, Ar-CH(CH₃)₂), 0.86 (d, *J* = 6.7 Hz, 6H, Ar-CH(CH₃)₂). ¹³C NMR (C₆D₆, 23 °C): δ 171.6 (Ar-CH=N), 162.4 (Ar-O-Ti), 152.8 (Ar-N=CH), 142.0 (Ar-C(CH₃)₃), 141.5 (Ar-C(CH₃)₃), 140.6 (Ar-CH₂-Ti), 138.4 (Ar-CH(CH₃)₂), 137.8 (C₇H₈), 132.2 (Ar-C), 131.7 (Ar-C), 129.7 (Ar-C), 129.3 (C₇H₈), 128.5 (Ar-C), 128.4 (C₇H₈), 127.5 (Ar-C), 125.7 (C₇H₈), 124.6 (Ar-C), 124.5 (Ar-C), 122.9 (Ar-C), 100.4 (Ar-CH₂-Ti), 35.6 (Ar-C(CH₃)₃), 34.3 (Ar-C(CH₃)₃), 31.4 (Ar-C(CH₃)₃), 30.5 (Ar-C(CH₃)₃), 29.2 (Ar-CH(CH₃)₂), 25.2 (Ar-CH(CH₃)₂), 23.0 (Ar-CH(CH₃)₂), 21.4 (C₇H₈).

Synthesis of [2,4-Br₂C₆H₂(O)(6-CH₂(NC₅H₉))CH₂N=CH-(2-adamantyl-4-MeC₆H₂OH)]Zr(Bn)₂ (3)

A solution of 2,4-Br₂C₆H₂(OH)(6-CH₂(NC₅H₉))CH₂N=CH-(2-adamantyl-4-MeC₆H₂OH) (0.50 g, 0.79 mmol) in toluene (15 mL) and Zr(Bn)₄ (0.36 g, 0.79 mmol) in toluene (15 mL) was pre-cooled at -30 °C inside the glovebox for 12 h. After mixing the solutions, an orange solution appeared instantly.

Stirring continued for 30 h at RT, after which the solvent was removed under reduced pressure to afford the crude product. This crude product contained some unreacted Zr(Bn)₄; it was washed with hexanes to remove Zr(Bn)₄ and further purified by crystallization from toluene at -30 °C to yield the pure product as an orange solid; yield: 0.36 g (50%). ¹H NMR (C₆D₆, 23 °C): δ 7.79 (s, 1H, CH=N), 7.40–7.29 (m, 6H, Ar-H), 7.11–6.83 (m, 8H, Ar-H, C₇H₈), 6.75–6.67 (m, 5H, Ar-H), 3.84–3.53 (br, 1H, Ar-CH₂), 3.43 (d, *J* = 8.7 Hz, 1H, Ar-CH₂), 3.35–3.21 (m, 1H, CH₂N=CH), 3.09–2.92 (bm, 1H, CH₂N=CH), 2.88–2.84 (bm, 1H, CH₂N), 2.74–2.59 (bm, 2H, CH₂N, CHN), 2.52 (bs, 6H, *adamantyl*), 2.26 (bs, 4H, Ar-CH₂-Zr), 2.24 (s, 3H, Ar-CH₃), 2.11 (s, 3H, C₇H₈), 2.07 (bs, 3H, *adamantyl*), 1.90–1.86 (bm, 6H, *adamantyl*), 1.31–1.19 (bm, 2H, CH₂), 1.12 (t, *J* = 6.9 Hz, 2H, CH₂), 0.97–0.91 (m, 1H, CH₂), 0.59 (t, *J* = 14.8 Hz, 1H, CH₂). ¹³C NMR (C₆D₆, 23 °C): δ 170.4 (CH=N), 167.8 (Ar-O-Zr), 166.5 (Ar-O-Zr), 158.4 (Ar-C), 157.5 (Ar-C), 154.4 (Ar-C), 148.9 (Ar-C), 139.7 (Ar-C), 137.9 (C₇H₈), 135.9 (Ar-C), 134.7 (Ar-C), 132.0 (Ar-C), 131.1 (Ar-C), 129.3 (C₇H₈), 129.2 (Ar-C), 128.7 (Ar-C), 128.5 (C₇H₈), 128.4 (Ar-C), 126.8 (Ar-C), 125.9 (Ar-C), 125.7 (C₇H₈), 125.5 (Ar-C), 123.5 (Ar-C), 120.0 (Ar-C), 119.4 (Ar-C), 113.8 (Ar-CH₂-Zr), 109.9 (Ar-CH₂-Zr), 68.0 (CHN), 65.7 (CH₂N=CH), 59.1 (CH₂N), 58.7 (Ar-CH₂), 48.03 (CH₂), 45.3 (CH₂), 40.9 (*adamantyl*), 37.5 (*adamantyl*), 29.7 (*adamantyl*), 29.6 (*adamantyl*), 23.0 (CH₂), 21.4 (Ar-CH₃), 20.9 (C₇H₈). This complex is highly sensitive towards air, moisture, light and heat, rendering it unsuitable for elemental analysis.

In situ generation, NMR data, and crystal structure of $[(2,6\text{-}^i\text{Pr}_2\text{C}_6\text{H}_3)\text{N}=\text{C}(3,5\text{-}^t\text{Bu}_2\text{C}_6\text{H}_2)\text{O}]\text{Zr}(\text{Bn})_2(\text{THF})^+[\text{BnB}(\text{C}_6\text{F}_5)_3]^-$ (4)

Cationic species 4 was generated by *in situ* mixing of 1 and B(C₆F₅)₃·THF in CD₂Cl₂ at ambient temperature, following the procedure for the clean and quantitative generation of cationic ester enolate *rac*-C₂H₄(1-indenyl)Zr⁺(THF)[OC(O^{*i*}Pr)=CMe₂]-[MeB(C₆F₅)₃]⁻.^{52,53} Specifically, in an argon-filled glovebox, a 4 mL glass vial was charged with 10 mg (0.011 mmol) of 1 and 0.4 mL of CD₂Cl₂, while another vial was charged with 6.87 mg of B(C₆F₅)₃·THF (0.011 mmol) and 0.4 mL of CD₂Cl₂. The two vials were mixed *via* a pipette at ambient temperature to give instantaneously a red solution, and subsequent NMR analysis showed the clean and quantitative formation of ion pair 4. ¹H NMR (CD₂Cl₂, 23 °C): δ 8.41 (s, 1H, CH=N), 7.99 (s, 1H, Ar-H), 7.41–7.36 (m, 2H, Ar-H), 7.28–7.14 (m, 11H, Ar-H, C₇H₈), 6.90–6.85 (m, 2H, Ar-H), 6.80–6.71 (m, 6H, Ar-H), 3.52–3.47 (m, 4H, α-CH₂ of THF), 2.80 (bs, 2H, Ar-CH(CH₃)₂), 2.34 (s, 3H, C₇H₈), 2.20–2.16 (m, 2H, Ar-CH₂-B), 2.09–2.02 (m, 4H, Ar-CH₂-Zr), 1.71–1.66 (m, 4H, β-CH₂ of THF), 1.60 (s, 9H, Ar-C(CH₃)₃), 1.39 (s, 9H, Ar-C(CH₃)₃), 1.14 (d, *J* = 6.7 Hz, 6H, Ar-CH(CH₃)₂), 0.89 (d, *J* = 6.6 Hz, 6H, Ar-CH(CH₃)₂). ¹⁹F NMR (CD₂Cl₂, 23 °C): δ -131.2 (m, 6F, *o*-F), -164.9 (t, *J*_{F-F} = 20.4 Hz, 3F, *p*-F), -167.7 (m, 6F, *m*-F).

The molecular structure of 4 has been confirmed by single crystal X-ray diffraction analysis. A 20 mL glass vial was charged with 10 mg (0.011 mmol) of 1, 6.87 mg of B(C₆F₅)₃·THF (0.011 mmol), and 3 mL of toluene. The

instantaneously formed red solution was carefully layered with 4 mL of hexanes and 0.5 mL of CH₂Cl₂. The vial was cooled to -30 °C and stored inside the glovebox freezer for 6 days to give orange single crystals of 4. After decanting the solvent, the crystals were quickly coated with a layer of Paratone-N oil (Exxon, dried and degassed at 140 °C/10⁻⁶ Torr for 16 h) in the glovebox. A crystal was then mounted on a thin glass fiber under a cold stream of dinitrogen gas. Single crystal X-ray diffraction data were acquired on a Bruker Kappa APEX II CCD diffractometer with Mo K_α radiation (λ = 0.71073 Å) and a graphite monochromator. Initial lattice parameters were obtained from a least-squares analysis of more than 100 reflections; these parameters were later refined against all data. The crystal did not show any significant decay during data collection. Data were integrated and corrected for Lorentz and polarization effects using Bruker APEX2 software, and semiempirical absorption corrections were applied using SCALE.⁵⁴ Space group assignments were based on systematic absences, *E* statistics, and successful refinement of the structure. The structure was solved by the Patterson method and refined with the aid of successive Fourier difference maps against all data using the SHELXTL 6.14 software package.⁵⁵ Thermal parameters for all non-hydrogen atoms were refined anisotropically, while all hydrogen atoms were assigned to ideal positions and refined using a riding model with an isotropic thermal parameter 1.2 times that of the attached carbon atom (1.5 times for methyl hydrogens). Selected bond distances and angles for compound 4 were collected in the caption of Fig. 2. All other metric parameters can be found in the cif file included with the ESI.† In the structure, C42 and C43 of the THF solvate molecule are disordered over two sites, with a site occupancy ratio refined to 40 : 60. In the structure the disordered toluene solvate molecule was found in Fourier difference maps to be disordered over multiple sites. After numerous attempts to model the disorder failed to improve agreement factors, SQUEEZE⁵⁶ was used to remove the disordered components. Selected crystallographic data for 4: C₇₀H₆₇BF₁₅NO₂Zr, triclinic, space group *P* $\bar{1}$, *a* = 10.9985(4) Å, *b* = 15.8569(6) Å, *c* = 20.4970(8) Å, α = 86.967(2)°, β = 75.119(2)°, γ = 73.850(2)°, *V* = 3317.8(2) Å³, *Z* = 2, *D*_{calcd} = 1.343 Mg m⁻³, GOF = 1.056, *R*₁ = 0.0580 [*I* > 2σ(*I*)], *wR*₂ = 0.1282. CCDC 924151 contains the supplementary crystallographic data.

In situ generation, NMR data and crystal structure of $[(2,6\text{-}^i\text{Pr}_2\text{C}_6\text{H}_3)\text{N}=\text{C}(3,5\text{-}^t\text{Bu}_2\text{C}_6\text{H}_2)\text{O}]\text{Ti}(\text{CH}_2\text{Ph})_2^+[\text{CH}_2\text{PhB}(\text{C}_6\text{F}_5)_3]^-$ (5)

Cationic species 5 was generated by *in situ* mixing of 2 and B(C₆F₅)₃·THF in CD₂Cl₂ at ambient temperature. In an argon-filled glovebox, a 4 mL glass vial was charged with 10 mg (0.012 mmol) of 2 and 0.4 mL of CD₂Cl₂, while another vial was charged with 7.23 mg of B(C₆F₅)₃·THF (0.012 mmol) and 0.4 mL of CD₂Cl₂. The two vials were mixed *via* a pipette at ambient temperature to give instantaneously a dark red solution, and subsequent NMR analysis showed the formation of ion pair 5 (major) with some additional minor species

((2,6-¹Pr₂C₆H₃)N=C(3,5-^tBu₂C₆H₂)O)Ti(CH₂Ph)₂(C₆F₅)(THF) and PhCH₂B(C₆F₅)₂. ¹H NMR (CD₂Cl₂, 23 °C) of the major species: δ 8.53 (s, 1H, CH=N), 8.08 (s, 1H, Ar-H), 7.47–7.38 (m, 2H, Ar-H), 7.28–7.11 (m, 11H, Ar-H, C₇H₈), 7.05–7.00 (m, 2H, Ar-H), 6.90–6.72 (m, 6H, Ar-H), 3.89 (bs, 4H, α-CH₂ of THF), 3.13–3.08 (m, 4H, Ar-CH₂-Ti), 3.03–3.00 (m, 2H, Ar-CH₂-B), 2.80 (bs, 2H, Ar-CH(CH₃)₂), 2.34 (s, 3H, C₇H₈), 1.72 (bs, 9H, Ar-C(CH₃)₃), 1.68 (bs, 4H, β-CH₂ of THF), 1.41 (s, 9H, Ar-C(CH₃)₃), 1.08 (d, *J* = 6.7 Hz, 6H, Ar-CH(CH₃)₂), 0.82 (d, *J* = 6.5 Hz, 6H, Ar-CH(CH₃)₂). ¹H NMR (CD₂Cl₂, 23 °C) of the minor species: δ 8.36 (s, CH=N), 7.78 (s, Ar-H), 7.28–7.11 (m, Ar-H), 6.90–6.72 (m, Ar-H), 4.08 (bs, α-CH₂ of THF), 3.13–3.08 (m, Ar-CH₂-Ti, Ar-CH₂-B), 2.92 (bs, Ar-CH(CH₃)₂), 2.08 (bs, β-CH₂ of THF), 1.53 (bs, Ar-C(CH₃)₃), 1.37 (s, Ar-C(CH₃)₃), 1.28 (d, *J* = 7.2 Hz, Ar-CH(CH₃)₂), 1.16 (d, *J* = 6.7 Hz, Ar-CH(CH₃)₂), 1.02 (d, *J* = 4.1 Hz, Ar-CH(CH₃)₂), 0.95 (d, *J* = 6.7 Hz, Ar-CH(CH₃)₂). ¹⁹F NMR (CD₂Cl₂, 23 °C) of the major species: δ -131.3 (m, 6F, *o*-F), -164.9 (t, *J*_{F-F} = 20.5 Hz, 3F, *p*-F), -167.8 (m, 6F, *m*-F). ¹⁹F NMR (CD₂Cl₂, 23 °C) of the minor species: δ -136.0 (m, *o*-F), -140.5 (m, *p*-F), -160.3 (m, *m*-F).

The molecular structure of **5** has been confirmed by single crystal X-ray diffraction analysis. A 20 mL glass vial was charged with 10 mg (0.012 mmol) of **2**, 7.23 mg of B(C₆F₅)₃·THF (0.012 mmol), and 3 mL of toluene. The resulting solution was carefully layered with 4 mL of hexanes. The vial was cooled to -30 °C and stored in the glovebox freezer for 12 days to afford single crystals of **5**. After decanting the solvent, the dark brownish crystals were quickly coated with a layer of Paratone-N oil (Exxon, dried and degassed at 140 °C/10⁻⁶ Torr for 16 h) in the glovebox. A crystal was then mounted on a thin glass fiber under a cold stream of dinitrogen gas. Single crystal X-ray diffraction data were acquired using the procedures already described for cation **4**. Selected bond distances and angles for compound **5** were collected in the caption of Fig. 3. All other metric parameters can be found in the cif file included in the ESI.† Selected crystallographic data for **5**: C₇₀H₆₇BF₁₅NO₂Ti, triclinic, space group *P* $\bar{1}$, *a* = 11.0260(4) Å, *b* = 15.5861(6) Å, *c* = 20.5604(8) Å, α = 84.504(2)°, β = 74.448(2)°, γ = 73.522(2)°, *V* = 3263.4(2) Å³, *Z* = 2, *D*_{calcd} = 1.365 Mg m⁻³, GOF = 1.026, *R*₁ = 0.0430 [*I* > 2σ(*I*)], w*R*₂ = 0.0882. CCDC 924152 contains the supplementary crystallographic data.

General polymerization procedures

Polymerizations were performed in 30 mL glass reactors in the glovebox in toluene or DMF at ambient temperature, following the procedure established for the polymerization of methacrylates and acrylamides by metallocene precatalysts.^{52,53,57} In a typical in-reactor activation polymerization procedure, the activator B(C₆F₅)₃ or B(C₆F₅)₃·THF (13.2 μmol) and 200 equiv. (2.64 mmol) of MMBL or MBL were premixed in 3 mL of toluene or DMF as indicated in the table. The polymerization was timed immediately after addition of precatalyst **1** to **3**. The pre-activation method (*i.e.*, premixing the neutral complex with an activator to generate the corresponding cationic catalyst, followed by addition of monomer to start the

polymerization) was also adopted in some runs for comparison. Similar procedures were followed in the case of MMA polymerization, except for neat polymerizations where the activator B(C₆F₅)₃ (39.6 μmol) and 400 equiv. of MMA (15.8 mmol) were premixed. After the measured time interval, a 0.2 mL aliquot was taken from the reaction mixture *via* a syringe and quickly quenched into a 4 mL vial containing 0.6 mL of undried “wet” CDCl₃ stabilized by 250 ppm of BHT-H; the quenched aliquots were later analyzed by ¹H NMR to obtain monomer conversion data. The polymerization was immediately quenched after the removal of the aliquot by adding 5 mL of 5% HCl-acidified methanol. The quenched mixture was precipitated into 100 mL of methanol, stirred for 3 h, filtered, and washed with methanol. The polymer collected was dried in a vacuum oven at 50 °C overnight to a constant weight.

Polymer characterizations

Polymer number-average molecular weights (*M*_n) and molecular weight distributions (MWD = *M*_w/*M*_n) were measured by gel permeation chromatography (GPC) analyses carried out at 40 °C and a flow rate of 1.0 mL min⁻¹, with DMF (for PMBL and PMMBL samples) or CHCl₃ (for PMMA) as the eluent, on a Waters University 1500 GPC instrument coupled with a Waters RI detector and equipped with four PLgel 5 μm mixed-C columns (Polymer Laboratories; linear range of molecular weight = 200–2 000 000). The instrument was calibrated with 10 PMMA standards, and chromatograms were processed with Waters Empower software. ¹H NMR and ¹³C NMR spectra for the analysis of PMMA,^{52,53} PMBL^{21,58} and PMMBL^{11,59} microstructures were recorded and analyzed according to the literature methods.

Results and discussion

Synthesis of neutral benzyl complexes 1–3

Protonolysis of tetrabenzyl precursors M(Bn)₄ (M = Zr, Ti) with equimolar 2,4-di-*tert*-butyl-6-((2,6-diisopropylphenylimino)methyl)phenol [(2,6-¹Pr₂C₆H₃)N=C(3,5-^tBu₂C₆H₂)OH] in toluene at -30 °C to 25 °C for 24 h yields the corresponding tribenzyl complexes **1** and **2** with concomitant liberation of the co-product toluene (Scheme 1). The Zr compound **1** was isolated in pure state as an orange solid by simple filtration of the resulting reaction mixture, followed by drying under vacuum for 1 h. Drying or standing at ambient temperature longer than 1 h resulted in a noticeable colour change from orange to yellow indicating decomposition, but the complex can be stored inside a -35 °C freezer without noticeable decomposition for an extended time period (up to a month). The Ti compound **2**, a red solid, was obtained by recrystallization of the crude product from toluene. Both complexes were isolated in good yield (~78%). Similarly, the 1 : 1 ratio reaction between Zr(Bn)₄ and the neutral salalen ligand, 2,4-Br₂C₆H₂(OH)-(6-CH₂(NC₅H₉))CH₂N=CH(2-adamantyl-4-MeC₆H₂OH), in toluene at -30 °C to 25 °C yielded dibenzyl **3** (Scheme 1). Isolation of the pure product (50% yield) was achieved through

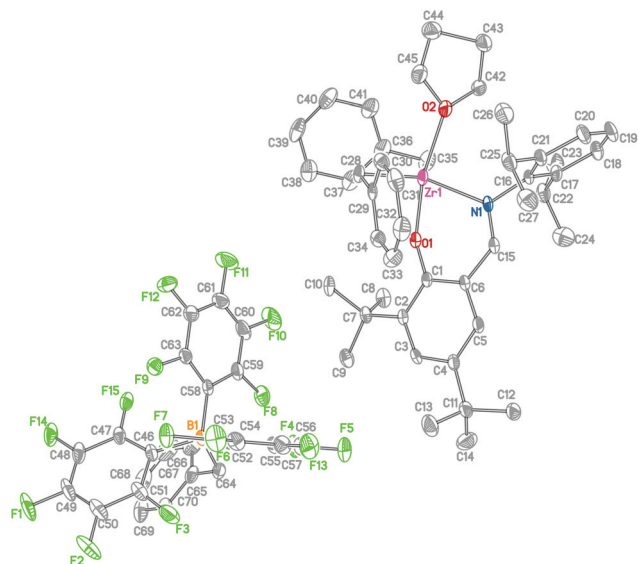


Fig. 2 X-ray crystal structure of $[(2,6\text{-}i\text{Pr}_2\text{C}_6\text{H}_3)\text{N}=\text{C}(3,5\text{-}t\text{Bu}_2\text{C}_6\text{H}_2)\text{O}]\text{Zr}(\text{Bn})_2(\text{THF})^+[\text{BnB}(\text{C}_6\text{F}_5)_3]^-$ (**4**) with thermal ellipsoids drawn at the 40% probability. Selected bond lengths (Å) and angles (°): Zr(1)–O(1), 1.9655(17); Zr(1)–O(2), 2.2529(19); Zr(1)–N(1), 2.3010(18); Zr(1)–C(28), 2.280(2); Zr(1)–C(35), 2.252(3); Zr(1)–C(36), 2.556(2); B(1)–C(64), 1.668(4); B(1)–C(58), 1.666(4); B(1)–C(46), 1.651(3); B(1)–C(52), 1.663(4); O(1)–Zr(1)–C(35), 95.87(10); O(1)–Zr(1)–O(2), 166.71(6); C(35)–Zr(1)–O(2), 90.68(10); O(1)–Zr(1)–C(28), 92.08(8); C(35)–Zr(1)–C(28), 124.97(9); O(2)–Zr(1)–C(28), 93.62(8); O(1)–Zr(1)–N(1), 78.74(6); C(35)–Zr(1)–N(1), 114.39(8); O(2)–Zr(1)–N(1), 88.03(7); C(28)–Zr(1)–N(1), 120.56(7); C(1)–O(1)–Zr(1), 142.60(14); C(15)–N(1)–Zr(1), 123.60(14); C(36)–C(35)–Zr(1), 83.95(14).

benzylborate anion $[\text{BnB}(\text{C}_6\text{F}_5)_3]^-$: δ –131.2 (m, 6F, *o*-F), –164.9 (t, 3F, *p*-F), –167.7 (m, 6F, *m*-F).

The solid-state structure of **4** (Fig. 2) was determined by single crystal X-ray diffraction analysis. The structure reveals unassociated cation–anion pairs. The zirconium center in the cation exhibits a distorted octahedral geometry furnished with η^2 -coordination of one benzyl group, η^1 -coordination of the other benzyl group, and the rest of the three coordination sites occupied by the side-arm imino nitrogen, the coordinated THF and the phenoxy oxygen. The Zr–C(benzyl) distances, Zr(1)–C(28), 2.280(2) Å, Zr(1)–C(35), 2.252(3) Å, match well with Zr–(OC₆HPh₂-2,6-Me₂-3,5)₂(CH₂Ph)[η^6 -C₆H₅CH₂B(C₆F₅)₃] [2.230(4) Å].^{48a,61} Bond distances of Zr(1)–N(1) = 2.3010(18) Å and Zr(1)–O(2) = 2.2529(19) Å indicate typical datively bonded N and O moieties, respectively. The η^2 -bonded benzyl group is characterized by a distance of Zr(1)–C(36) = 2.556(2) Å and a bond angle of C(36)–C(35)–Zr(1) = 83.95(14)°. The two coordinated hetero atoms and the η^2 -bonded benzyl group play a key role to stabilize the octahedral cationic zirconium center $[(2,6\text{-}i\text{Pr}_2\text{C}_6\text{H}_3)\text{N}=\text{C}(3,5\text{-}t\text{Bu}_2\text{C}_6\text{H}_2)\text{O}]\text{Zr}(\text{Bn})_2(\text{THF})^+$, which avoid back π -bonding (η^6 -coordination) of the abstracted benzyl group $[\text{BnB}(\text{C}_6\text{F}_5)_3]^-$ to the cationic Zr center. The acute angles of C(29)–C(28)–Zr(1), 102.96(13)°, C(36)–C(35)–Zr(1), 83.95(14)° indicate the phenyl rings of both benzyl groups bent towards the zirconium center, but Zr(1)–C(28) benzyl is best described as the η^1 -benzyl bond [Zr(1)–C(29) = 2.986(2) Å]. The bond angles, O(1)–Zr(1)–C(35), 95.87(10)°,

O(1)–Zr(1)–O(2), 166.71(6)°, C(35)–Zr(1)–O(2), 90.68(10)°, O(1)–Zr(1)–C(28), 92.08(8)°, C(35)–Zr(1)–C(28), 124.97(9)°, and O(2)–Zr(1)–C(28), 93.62(8)°, collaborate with the distorted octahedral Zr center.

Cationic species $[(2,6\text{-}i\text{Pr}_2\text{C}_6\text{H}_3)\text{N}=\text{C}(3,5\text{-}t\text{Bu}_2\text{C}_6\text{H}_2)\text{O}]\text{Ti}(\text{Bn})_2(\text{THF})^+[\text{BnB}(\text{C}_6\text{F}_5)_3]^-$ (**5**) was generated in the same manner as for generation of **4**, but in the case of the Ti cation **5**, its formation was accompanied by formation of two additional species due to decomposition *via facile* C₆F₅ ligand transfer^{48a,48e,48f} (*vide infra*). Prolonged storage (>2 h) in CD₂Cl₂ at room temperature resulted in complete decomposition. Attempts to generate the base-free cation using B(C₆F₅)₃ led to formation of unidentifiable decomposition products. Two individual sets of signals were observed for Ar–CH₂–B, Ar–CH₂–Ti methylene protons in the expected ratio of 1:2 (δ 3.03–3.13). As in the Zr cation **4**, two different doublets (δ 1.08, 0.82) were also observed for Ar–CH(CH₃)₂ in the Ti cation **5**. ¹⁹F NMR clearly shows formation of benzylborate anion $[\text{BnB}(\text{C}_6\text{F}_5)_3]^-$: δ –131.3 (m, 6F, *o*-F), –164.9 (t, 3F, *p*-F), –167.8 (m, *m*-F). Two additional species were identified as $(2,6\text{-}i\text{Pr}_2\text{C}_6\text{H}_3)\text{N}=\text{C}(3,5\text{-}t\text{Bu}_2\text{C}_6\text{H}_2)\text{O}]\text{Ti}(\text{CH}_2\text{Ph})_2(\text{C}_6\text{F}_5)(\text{THF})$ and $\text{PhCH}_2\text{B}(\text{C}_6\text{F}_5)_2$, decomposition products *via* transfer of the C₆F₅ ligand from the borate anion to the Ti cation.

The solid-state structure of **5** (Fig. 3) was determined by single crystal X-ray diffraction analysis. The structure reveals unassociated cation–anion pairs. As in the cation of **4**, the titanium center in the cation of **5** exhibits a distorted octahedral

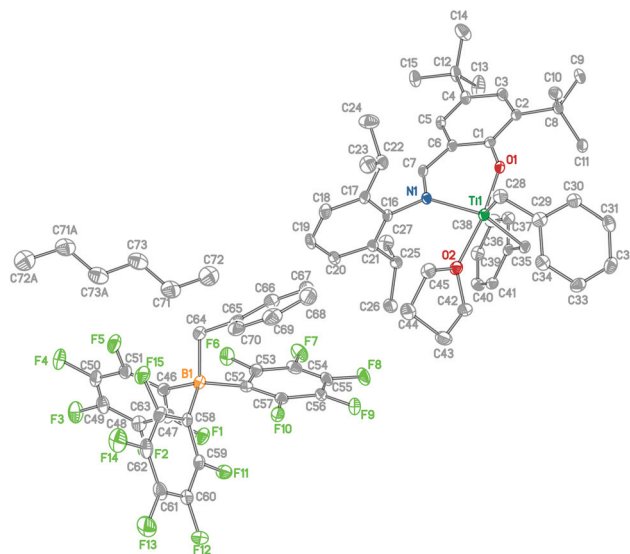


Fig. 3 X-ray crystal structure of $[(2,6\text{-}i\text{Pr}_2\text{C}_6\text{H}_3)\text{N}=\text{C}(3,5\text{-}t\text{Bu}_2\text{C}_6\text{H}_2)\text{O}]\text{Ti}(\text{Bn})_2(\text{THF})^+[\text{BnB}(\text{C}_6\text{F}_5)_3]^-$ (**5**) with thermal ellipsoids drawn at the 40% probability. Selected bond lengths (Å) and angles (°): Ti(1)–O(1), 1.8320(16); Ti(1)–O(2), 2.1114(17); Ti(1)–N(1), 2.1613(18); Ti(1)–C(28), 2.119(2); Ti(1)–C(29), 2.548(2); Ti(1)–C(35), 2.156(2); B(1)–C(64), 1.656(4); B(1)–C(58), 1.671(4); B(1)–C(46), 1.672(3); B(1)–C(52), 1.649(4); O(1)–Ti(1)–C(35), 91.30(8); O(1)–Ti(1)–O(2), 171.13(6); C(35)–Ti(1)–O(2), 93.69(8); O(1)–Ti(1)–C(28), 93.93(9); C(35)–Ti(1)–C(28), 121.33(9); O(2)–Ti(1)–C(28), 89.73(9); O(1)–Ti(1)–N(1), 83.47(7); C(35)–Ti(1)–N(1), 119.38(8); O(2)–Ti(1)–N(1), 87.69(7); C(28)–Ti(1)–N(1), 119.27(8); C(1)–O(1)–Ti(1), 142.14(14); C(7)–N(1)–Ti(1), 122.31(15); C(29)–C(28)–Ti(1), 88.68(15).

geometry furnished with η^2 -coordination of one benzyl group, η^1 -coordination of the other benzyl group, and the rest of the three coordination sites occupied by the side-arm imino nitrogen, the coordinated THF, and the phenoxy oxygen. The Ti–C (benzyl) distances, Ti(1)–C(28), 2.119(2) Å, Ti(1)–C(35), 2.156(2) Å, match well with Ti(OC₆H₃Ph₂-2,6)₂(CH₂Ph)[η^6 -C₆H₅CH₂B(C₆F₅)₃] [2.159(9) Å].^{48a} Bond distances of Ti(1)–N(1) = 2.1613(18) Å and Ti(1)–O(2) = 2.1114(17) Å indicate typical datively bonded N and O moieties, respectively. The η^2 -bonded benzyl group is characterized by a distance of Ti(1)–C(29) = 2.548(2) and a bond angle of C(29)–C(28)–Ti(1) = 88.68(15)°. Like the cationic Zr complex **4**, two coordinated hetero atoms and one η^2 -bonded benzyl group in **5** play a key role to stabilize the octahedral cationic titanium center, which avoid back π -bonding (η^6 -coordination) of the abstracted benzyl group ([BnB(C₆F₅)₃]⁺) to the cationic titanium center. The acute angles of C(29)–C(28)–Ti(1), 88.68(15)°, C(36)–C(35)–Ti(1), 110.14(14)° indicate phenyl rings of both benzyl groups bent towards the titanium center, but Ti(1)–C(35) benzyl is best described as the η^1 -benzyl bond [Ti(1)–C(36) = 3.003(2) Å]. The bond angles, O(1)–Ti(1)–C(35), 91.30(8)°, O(1)–Ti(1)–O(2), 171.13(6)°, C(35)–Ti(1)–O(2), 93.69(8)°, O(1)–Ti(1)–C(28), 93.93(9)°, C(35)–Ti(1)–C(28), 121.33(9)°, and O(2)–Ti(1)–C(28), 89.73(9)°, collaborate with the distorted octahedral cationic titanium center.

Polymerization of MMBL by catalysts derived from complexes 1–3

Control runs using the activators, B(C₆F₅)₃ or B(C₆F₅)₃·THF, and precatalysts, neutral complexes 1–3, individually for polymerization of MMBL (200 equiv.) at RT in toluene or DMF yielded no polymer formation up to 24 h. Worth noting here is that coordination-addition polymerization of acrylic monomers by cationic group 4 metallocenium catalysts was typically carried out in nonpolar hydrocarbons such as toluene or polar non-coordinating solvents such as CH₂Cl₂, while polar coordinating solvents such as THF and DMF usually inhibit the polymerization.²⁷ Owing to insolubility of PMMBL in toluene, polymerization of MMBL by group 4 catalysts in this solvent proceeds in a heterogeneous fashion, negatively impacting the

catalyst activity and polymerization control. Nevertheless, the polymerization of MMBL (200 equiv.) in toluene by **1** and **B** (C₆F₅)₃ using the in-reactor activation protocol achieved quantitative monomer conversion (99% isolated polymer yield) after 24 h. The resulting atactic PMMBL (51.8% mr) exhibited a relatively broad MWD with PDI = 2.19 and the measured M_n of 5.06×10^4 g mol⁻¹ was much higher than the calculated one, thus giving rise to a low initiator efficiency of $I^* = 44\%$ (run 1, Table 1). Increasing the [MMBL]/[**1**] ratio to 400 brought about much higher molecular weight of the resulting PMMBL ($M_n = 8.59 \times 10^4$ g mol⁻¹, run 2, Table 1) although the polymerization achieved only 60% isolated polymer yield during the same time period (24 h). The polymerization in toluene using the pre-activation method (*i.e.*, pre-mixing **1** with B(C₆F₅)₃·THF to generate the corresponding cationic catalyst before addition of monomer) gave similar polymerization results to those obtained by the in-reactor activation procedure (run 4 *vs.* run 1, Table 1). On the other hand, the polymerization in DMF by the pre-activation method afforded only 26% polymer yield although the polymer molecular weight was still similar ($M_n = 5.43 \times 10^4$ g mol⁻¹, PDI = 2.81, $I^* = 10\%$, run 3, Table 1). In comparison, polymerizations by in-reactor activation of complex **2** in toluene achieved higher initiator efficiencies, up to 90% (runs 5–7, Table 1), and afforded syndio-biased polymers (47.8% rr to 57.0% rr). The MMBL polymerization by in-reactor activation of the unsymmetric complex **3** with B(C₆F₅)₃ achieved quantitative monomer conversion (99% isolated yield) but the resulting polymer was still only syndio-biased (61.2% rr, 30.6% mr, run 8, Table 1).

Polymerization of MBL by catalysts derived from complexes 1–3

Controlling the stereochemistry of MBL polymerization has been a challenge. For example, MBL polymerization by a *C_s*-ligated zirconocene catalyst, {[*p*-Et₃SiPh)₂C(Cp)(2,7-^tBu₂-Flu)]-Zr[OC(OⁱPr)=CMeCH₂C(Me)₂C(OⁱPr)=O]}⁺[B(C₆F₅)₄]⁻, which has been shown to be a highly active and syndiospecific polymerization catalyst for MMA polymerization,^{57a} resulted in only a modest polymer yield of 40% and a syndio-biased atactic polymer (50.8% rr, 23.1% mr). On the other hand, near

Table 1 Selected results of MMBL polymerization by complexes 1–3^a

Run no.	Complex	Activator	MMBL/ complex	Solvent	Isolated yield (%)	$10^{-4} M_n^b$ (g mol ⁻¹)	PDI ^b (M_w/M_n)	I^*^c (%)	[rr] ^d (%)	[mr] ^d (%)	[mm] ^d (%)
1	1	B(C ₆ F ₅) ₃	200	Toluene	99	5.06	2.19	44	36.5	51.8	11.7
2	1	B(C ₆ F ₅) ₃	400	Toluene	60	8.59	2.62	31	42.7	47.3	10.0
3	1	B(C ₆ F ₅) ₃	200	DMF	26	5.43	2.81	10	n.d.	n.d.	n.d.
4	1	B(C ₆ F ₅) ₃ ·THF	200	Toluene	98	5.78	2.40	38	n.d.	n.d.	n.d.
5	2	B(C ₆ F ₅) ₃	200	Toluene	98	3.21	2.03	68	47.8	39.7	12.5
6	2	B(C ₆ F ₅) ₃	400	Toluene	63	3.14	2.02	90	57.0	33.2	9.8
7	2	B(C ₆ F ₅) ₃	200	DMF	98	4.88	1.98	45	n.d.	n.d.	n.d.
8	3	B(C ₆ F ₅) ₃	200	Toluene	99	7.75	3.39	28	61.2	30.6	8.2

^a Conditions: [complex]/[activator] = 1; solvent = 3 mL; temperature = 25 °C; time = 24 h; monomer was pre-mixed with the activator followed by addition of complex (*i.e.*, in-reactor activation), except for runs 3, 4 and 8 where complexes were pre-activated with an activator followed by addition of monomer (*i.e.*, pre-activation); n.d. = not determined. ^b Number-average molecular weight (M_n) and polydispersity index (PDI) determined by GPC relative to PMMA standards. ^c Initiator efficiency (I^*) = $M_n(\text{calcd})/M_n(\text{exptl})$, where $M_n(\text{calcd}) = \text{MW}(\text{monomer}) \times [\text{monomer}]/[\text{catalyst}] \times \text{conversion\%} + \text{MW of chain-end groups}$. ^d Tacticity measured by ¹³C NMR spectroscopy with DMSO-d₆ as a solvent at 100 °C.

Table 2 Selected results of MBL polymerization by complexes 1–3^a

Run no.	Complex	Activator	MBL/complex	Isolated yield (%)	$10^{-4} M_n$ (g mol ⁻¹)	PDI (M_w/M_n)	I^* (%)	[rr] (%)	[mr] (%)	[mm] (%)
1	1	B(C ₆ F ₅) ₃	200	96	4.85	2.99	39	49.2	30.4	20.4
2	1	B(C ₆ F ₅) ₃ ·THF	200	96	2.01	2.40	94	n.d.	n.d.	n.d.
3	2	B(C ₆ F ₅) ₃	200	87	2.35 ^b	4.13 ^b	73	39.3	31.7	29.0
4	3	B(C ₆ F ₅) ₃	200	99	5.57	3.11	35	49.0	33.1	17.9

^a Conditions: [complex]/[activator] = 1; solvent (toluene) = 3 mL; temperature = 25 °C; time = 24 h; monomer was pre-mixed with the activator followed by addition of complex (*i.e.*, in-reactor activation), except for runs 2 and 4 where complexes were pre-activated with an activator followed by addition of monomer (*i.e.*, pre-activation). See footnotes under Table 1 for other abbreviations or explanations. ^b There was a minor (~2%), higher MW shoulder peak.

quantitative polymer yield (96%) can be achieved by the catalyst system based on complex 1 using either in-reactor activation with B(C₆F₅)₃ (run 1, Table 2) or pre-activation with B(C₆F₅)₃·THF (run 2, Table 2), although the latter polymerization approach exhibited a much higher initiator efficiency (94%) than the former method (39%). The resulting PMBL is, however, also a syndio-biased atactic material (49.2% *rr*, 30.4% *mr*, run 1, Table 2), so is the polymer produced by the catalyst based on the Ti complex 2 (39.3% *rr*, 31.7% *mr*, run 3, Table 2). Again, the chiral catalyst based on the unsymmetric complex 3 also led to a syndio-biased atactic polymer (49.0% *rr*, 33.1% *mr*, run 4, Table 2).

As controls, we also examined the performance of the catalysts derived from benzyl complexes 1–3 for polymerization of MMA (200 equiv.) at RT in toluene, CH₂Cl₂, or neat. Under these conditions, the polymerizations by all three catalysts were sluggish, achieving less than 20% monomer conversion even after 24 h. The PMMAs produced are syndio-rich atactic materials, with the one produced by the catalyst based on the Zr complex 1 in neat conditions exhibiting the highest syndio-tacticity of 83.4% *rr*, followed by the PMMA (71.5% *rr*) produced by the catalyst derived from the Ti complex 2. The catalyst system based on the C₁-symmetric 3 also led to syndio-rich polymers, with syndiotacticity ranging from 68.5% to 73.2% *rr*, depending on the reaction medium (in toluene, CH₂Cl₂, or neat). Overall, these non-metallocene-based cationic catalysts are considerably less active, stereoselective, and controlled, as compared to metallocene-based cationic catalysts.²⁷

Conclusions

In summary, we have employed the protonolysis route to synthesize new (imino)phenoxy and salalen group 4 benzyl complexes 1–3, which were isolated under ambient conditions in good yields. Activation of tribenzyl complexes 1 (Zr) and 2 (Ti) with B(C₆F₅)₃·THF in CD₂Cl₂ led to formation of the corresponding cationic dibenzyl complexes 4 (Zr) and 5 (Ti), which were characterized by NMR and X-ray diffraction analysis. To the best of our knowledge, complexes 4 and 5 are the first examples of the structurally characterized (imino)phenoxy group 4 dibenzyl cations to date. These hexa-coordinate

cationic metal centers are stabilized by the side-arm (imino)phenoxy nitrogen donor atom, coordinated THF, and the η²-bonded benzyl group. This mode of stabilization is different from the commonly observed back binding (η⁶-coordination) of the benzyl group abstracted to the anion.

These three benzyl complexes, upon appropriate activation (in-reactor or pre-activation method, or both), have been investigated for their activity and stereoselectivity towards polymerization of renewable monomers MBL and MMBL. High to quantitative polymer yields can be achieved under certain conditions, but the resulting polymers typically exhibit relatively broad molecular weight distributions and essentially atactic or syndio-biased atactic microstructures. This trend holds true even for the chiral catalyst derived from activation of the unsymmetric complex 3. These results, coupled with the control run results obtained from MMA polymerization, indicate that the herein investigated non-metallocene-based catalysts are considerably less active, stereoselective, and controlled in coordination polymerization of conjugated polar alkenes such as MMA, MBL, and MMBL, than group 4 metallocene or lanthanocene-based catalysts.

Acknowledgements

This work was supported by the National Science Foundation (NSF-1012326). We thank Boulder Scientific Co. for the research gift of B(C₆F₅)₃, Dr Yuetao Zhang for GPC analysis of PMMBL, PMBL and PMMA, and Dr Brian S. Newell for the help on the X-ray structural analysis.

References

- 1 C. K. Williams and M. A. Hillmyer, Polymers from renewable resources: a perspective for a special issue of polymer reviews, *Polym. Rev.*, 2008, **48**, 1–10.
- 2 M. A. R. Meier, J. O. Metzger and U. S. Schubert, Plant oil renewable resources as green alternatives in polymer science, *Chem. Soc. Rev.*, 2007, **36**, 1788–1802.
- 3 (a) G. W. Coates and M. A. Hillmyer, A virtual issue on “Polymers from renewable resources”, *Macromolecules*, 2009, **42**, 7987–7989; (b) A. Gandini, Polymers from renewable resources: a challenge for the future of

- macromolecular materials, *Macromolecules*, 2008, **41**, 9491–9504; (c) A. H. Tullo, Growing plastics, *Chem. Eng. News*, 2008, **86**(39), 21–25.
- 4 M. W. P. C. V. Rossum, M. Alberda and L. H. W. V. D. Plas, *Phytochemistry*, 1998, **49**, 723–729.
- 5 H. M. R. Hoffman and J. Rabe, *Angew. Chem., Int. Ed. Engl.*, 1985, **24**, 94–110.
- 6 C. J. Brandenburg, *US Pat.*, 6 841 627 B2, 2005.
- 7 M. K. Akkapeddi, *Macromolecules*, 1979, **12**, 546–551.
- 8 J. E. Pickett and Q. Ye, *US Pat.*, 2007/0122625, 2007.
- 9 L. E. Manzer, *ACS Symp. Ser.*, 2006, **921**, 40–51.
- 10 L. E. Manzer, *Appl. Catal., A*, 2004, **272**, 249–256.
- 11 R. Mullin, Sustainable specialties, *Chem. Eng. News*, 2004, **82**(45), 29–37.
- 12 (a) M. K. Akkapeddi, *Polymer*, 1979, **20**, 1215–1216; (b) J. W. Stansbury and J. M. Antonucci, *Dent. Mater.*, 1992, **8**, 270–273; (c) J. Mosnáček, J. A. Yoon, A. Juhari, K. Koynov and K. Matyjaszewski, *Polymer*, 2009, **50**, 2087–2094; (d) J. Mosnáček and K. Matyjaszewski, *Macromolecules*, 2008, **41**, 5509–5511; (e) M. Ueda, M. Takahashi, Y. Imai and C. U. Pittman Jr., *J. Polym. Sci., Polym. Chem. Ed.*, 1982, **20**, 2819–2828; (f) A. A. Gridnev and S. D. Ittel, *WO 035960 A2*, 2000.
- 13 D. Y. Sogah, W. R. Hertler, O. W. Webster and G. M. Cohen, *Macromolecules*, 1987, **20**, 1473–1488.
- 14 G. M. Miyake, S. E. Newton, W. R. Mariott and E. Y.-X. Chen, *Dalton Trans.*, 2010, **39**, 6710–6718.
- 15 M. van den Brink, W. Smulders, A. M. van Herk and A. L. German, *J. Polym. Sci., Polym. Chem. Ed.*, 1999, **37**, 3804–3816.
- 16 H. Koinuma, K. Sato and H. Hirai, *Makromol. Chem., Rapid Commun.*, 1982, **3**, 311–315.
- 17 C. Lee and H. K. Hall Jr., *Macromolecules*, 1989, **22**, 21–25.
- 18 D. L. Trumbo, *Polym. Bull.*, 1991, **26**, 271–275.
- 19 G. Qi, M. Nolan, F. J. Schork and C. W. Jones, *J. Polym. Sci., Polym. Chem. Ed.*, 2008, **46**, 5929–5944.
- 20 J. Suenaga, D. M. Sutherland and J. K. Stille, *Macromolecules*, 1984, **17**, 2913–2916.
- 21 G. M. Miyake, Y. Zhang and E. Y.-X. Chen, *Macromolecules*, 2010, **43**, 4902–4908.
- 22 Y. Hu, X. Xu, Y. Zhang, Y. Chen and E. Y.-X. Chen, *Macromolecules*, 2010, **43**, 9328–9336.
- 23 (a) Y. Zhang, G. M. Miyake and E. Y.-X. Chen, *Angew. Chem., Int. Ed. Engl.*, 2010, **49**, 10158–10162; (b) Y. Zhang, G. M. Miyake, M. G. John, L. Falivene, L. Caporaso, L. Cavallo and E. Y.-X. Chen, *Dalton Trans.*, 2012, **41**, 9119–9134.
- 24 Y. Zhang, L. O. Gustafson and E. Y.-X. Chen, *J. Am. Chem. Soc.*, 2011, **133**, 13674–13684.
- 25 Y. Zhang and E. Y.-X. Chen, *Angew. Chem., Int. Ed. Engl.*, 2012, **51**, 2465–2469.
- 26 X. Chen, L. Caporaso, L. Cavallo and E. Y.-X. Chen, *J. Am. Chem. Soc.*, 2012, **134**, 7278–7281.
- 27 E. Y.-X. Chen, *Chem. Rev.*, 2009, **109**, 5157–5214.
- 28 (a) G. J. P. Britovsek, V. C. Gibson and D. F. Wass, *Angew. Chem., Int. Ed. Engl.*, 1999, **38**, 428–447; (b) V. C. Gibson and S. K. Spitzmesser, *Chem. Rev.*, 2003, **103**, 283–315; (c) G. W. Coates, *J. Chem. Soc., Dalton Trans.*, 2002, 467–475; (d) G. W. Coates, P. D. Hustad and S. Reinartz, *Angew. Chem., Int. Ed. Engl.*, 2002, **41**, 2236–2257; (e) M. Lamberti, M. Mazzeo, D. Pappalardo and C. Pellicchia, *Coord. Chem. Rev.*, 2009, **253**, 2082–2097; (f) M. Delferro and T. J. Marks, *Chem. Rev.*, 2011, **111**, 2450–2485.
- 29 A. van der Linden, C. J. Schaverien, N. Meijboom, C. Ganter and A. G. Orpen, *J. Am. Chem. Soc.*, 1995, **117**, 3008–3021.
- 30 R. Baumann, W. M. Davis and R. R. Schrock, *J. Am. Chem. Soc.*, 1997, **119**, 3830–3831.
- 31 Y.-M. Jeon, S. J. Park, J. Heo and K. Kim, *Organometallics*, 1998, **17**, 3161–3163.
- 32 Z. Ziniuk, I. Goldberg and M. Kol, *Inorg. Chem. Commun.*, 1999, **2**, 549–551.
- 33 E. Y. Tshuva, I. Goldberg and M. Kol, *J. Am. Chem. Soc.*, 2000, **122**, 10706–10707.
- 34 E. Y. Tshuva, I. Goldberg, M. Kol and Z. Goldschmidt, *Chem. Commun.*, 2001, 2120–2121.
- 35 E. Y. Tshuva, I. Goldberg and M. Kol, *Organometallics*, 2001, **20**, 3017–3028.
- 36 E. Y. Tshuva, S. Groysman, I. Goldberg, M. Kol and Z. Goldschmidt, *Organometallics*, 2002, **21**, 662–670.
- 37 (a) S. Groysman, I. Goldberg, M. Kol, E. Genizi and Z. Goldschmidt, *Inorg. Chim. Acta*, 2003, **345**, 137–144; (b) S. Groysman, I. Goldberg, M. Kol, E. Genizi and Z. Goldschmidt, *Organometallics*, 2003, **22**, 3013–3015.
- 38 S. Segal, I. Goldberg and M. Kol, *Organometallics*, 2005, **24**, 200–202.
- 39 (a) A. Yeori, I. Goldberg, M. Shuster and M. Kol, *J. Am. Chem. Soc.*, 2006, **128**, 13062–13063; (b) A. Yeori, I. Goldberg and M. Kol, *Macromolecules*, 2007, **40**, 8521–8523; (c) A. Cohen, A. Yeori, J. Kopilov, I. Goldberg and M. Kol, *Chem. Commun.*, 2008, 2149–2151.
- 40 S. Gendler, A. L. Zelikoff, J. Kopilov, I. Goldberg and M. Kol, *J. Am. Chem. Soc.*, 2008, **130**, 2144–2145.
- 41 S. Segal, A. Yeori, M. Shuster, Y. Rosenberg and M. Kol, *Macromolecules*, 2008, **41**, 1612–1617.
- 42 A. Cohen, J. Kopilov, I. Goldberg and M. Kol, *Organometallics*, 2009, **28**, 1391–1405.
- 43 K. Press, A. Cohen, I. Goldberg, V. Venditto, M. Mazzeo and M. Kol, *Angew. Chem., Int. Ed. Engl.*, 2011, **50**, 3529–3532.
- 44 G.-J. M. Meppelder, H.-T. Fan, T. P. Spaniol and J. Okuda, *Organometallics*, 2009, **28**, 5159–5165.
- 45 (a) E. T. Kiesewetter, S. Randoll, M. Radlauer and R. M. Waymouth, *J. Am. Chem. Soc.*, 2010, **132**, 5566–5567; (b) S. Randoll, E. T. Kiesewetter and R. M. Waymouth, *J. Polym. Sci., Part A: Polym. Chem.*, 2012, **50**, 2604–2611.
- 46 (a) R. R. Gowda, D. Chakraborty and V. Ramkumar, *Eur. J. Inorg. Chem.*, 2009, 2981–2993; (b) T. K. Saha, B. Rajashekhar, R. R. Gowda, V. Ramkumar and D. Chakraborty, *Dalton Trans.*, 2010, **39**, 5091–5093; (c) T. K. Saha, B. Rajashekhar and D. Chakraborty, *RSC Adv.*, 2012, **2**, 307–318; (d) T. K. Saha, M. Mandal,

- D. Chakraborty and V. Ramkumar, *New J. Chem.*, 2013, **37**, 949–960.
- 47 (a) D. A. Pennington, D. L. Hughes, M. Bochmann and S. J. Lancaster, *Dalton Trans.*, 2003, 3480–3482; (b) D. A. Pennington, W. Clegg, S. J. Coles, R. W. Harrington, M. B. Hursthouse, D. L. Hughes, M. E. Light, M. Schormann, M. Bochmann and S. J. Lancaster, *Dalton Trans.*, 2005, 561–571.
- 48 (a) M. G. Thorn, Z. C. Etheridge, P. E. Fanwick and I. P. Rothwell, *J. Org. Chem.*, 1999, **591**, 148–162; (b) E. Y.-X. Chen and T. J. Marks, *Chem. Rev.*, 2000, **100**, 1391–1434; (c) S. Groysman, E. Sergeeva, I. Goldberg and M. Kol, *Inorg. Chem.*, 2005, **44**, 8188–8190; (d) M. G. Thorn, Z. C. Etheridge, P. E. Fanwick and I. P. Rothwell, *Organometallics*, 1998, **17**, 3636–3638; (e) J. D. Scollard, D. H. McConville and S. J. Rettig, *Organometallics*, 1997, **16**, 1810–1812; (f) K. Phomphrai, A. E. Fenwick, S. Sharma, P. E. Fanwick, J. M. Caruthers, W. N. Delgass, M. M. Abu-Omar and I. P. Rothwell, *Organometallics*, 2006, **25**, 214–220.
- 49 U. Zucchini, E. Alizzati and U. J. Giannini, *J. Organomet. Chem.*, 1971, **26**, 357–372.
- 50 K.P. Bryliakov and E. P. Talsi, *Eur. J. Org. Chem.*, 2008, 3369–3376.
- 51 P. A. Cameron, V. C. Gibson, C. Redshaw, J. A. Segal, G. A. Solan, A. J. P. White and D. J. Williams, *J. Chem. Soc., Dalton Trans.*, 2001, 1472–1476.
- 52 A. D. Bolig and E. Y.-X. Chen, *J. Am. Chem. Soc.*, 2004, **126**, 4897–4906.
- 53 A. Rodriguez-Delgado and E. Y.-X. Chen, *Macromolecules*, 2005, **38**, 2587–2594.
- 54 G. Sheldrick, *SADABS*, Bruker AXS: Madison, WI, 1997.
- 55 G. Sheldrick, *SHELXTL*, 6.14, Bruker AXS: Madison, WI, 2004.
- 56 A. L. Spek, *J. Appl. Crystallogr.*, 2003, **36**, 7–13.
- 57 (a) Y. Zhang, Y. Ning, L. Caporaso, L. Cavallo and E. Y.-X. Chen, *J. Am. Chem. Soc.*, 2010, **132**, 2695–2709; (b) W. R. Mariott and E. Y.-X. Chen, *Macromolecules*, 2005, **38**, 6822–6832.
- 58 (a) M. K. Akkapeddi, *Macromolecules*, 1979, **12**, 546–551; (b) D. Y. Sogah, W. R. Hertler, O. W. Webster and G. M. Cohen, *Macromolecules*, 1987, **20**, 1473–1488.
- 59 J. Suenaga, D. M. Sutherlin and J. K. Stille, *Macromolecules*, 1984, **17**, 2913–2916.
- 60 E. Kirillov, T. Roisnel and J.-F. Carpentier, *Organometallics*, 2012, **31**, 3228–3240.
- 61 C. Pellecchia, A. Grassi and A. Immirzi, *J. Am. Chem. Soc.*, 1993, **115**, 1160–1162.